Materials Letters 64 (2010) 1271–1274

Contents lists available at ScienceDirect

Materials Letters

journal homepage: www.elsevier.com/locate/matlet

Synthesis of CoNi nanowires by heterogeneous nucleation in polyol

Qiying Liu [a,b], Xiaohui Guo [a], Tiejun Wang [b], Yong Li [a], Wenjie Shen [a,*]

[a] State Key Laboratory of Catalysis, Dalian Institute of Chemical Physics, Chinese Academy of Sciences, Dalian 116023, China
[b] Key Laboratory of Renewable Energy and Gas Hydrate, Guangzhou Institute of Energy Conversion, Chinese Academy of Sciences, Guangzhou 510640, China

ARTICLE INFO

Article history:
Received 9 January 2010
Accepted 2 March 2010
Available online 6 March 2010

Keywords:
Metallic alloys
CoNi nanowires
Crystal growth
Core-shell structure
Shape control

ABSTRACT

CoNi nanorwires/nanorods, depending on the loading of Ni, were prepared by heterogeneous nucleation in polyol. CoNi nanowires with the length up to 1000 nm and the diameter of about 10 nm were obtained when the loading of Ni was no more than 30%, whereas nanorods with the length of about 500 nm and the diameter of 20 nm were produced with further increasing the loading of Ni. It was revealed that the nanowires might be a core-shell structure where the core was formed by the fast reduction of Co^{2+} and the shell was constructed by the combined reduction of Co^{2+} and Ni^{2+}. When used for hydrogenolysis of glycerol, the CoNi nanowires showed significantly enhanced glycerol conversion and propanediol selectivity as compared to the pure Co nanowires.

1. Introduction

Bimetallic nanomaterials have attracted wide attention because of their unique properties which are largely different from their monometal counterparts [1,2]. Doping a second metal in transition metals could adjust the d-band filling of electron, and thus greatly alter the surface properties as well as the catalytic performance [3,4]. For example, NiAu alloy showed excellent activity and stability in steam reforming of n-butane, where the doping of Au decreased the activation energy for C–H bond and thus impeded coke deposition [5]. CuPt alloy exhibited exceptionally high activity in low-temperature water–gas-shift reaction because of the facile activation of H_2O and the weak adsorption of CO [6]. CoNi alloy was also found to be highly active for methane drying reforming, and the alloyed structure significantly promoted the stability by inhibiting coke formation [7,8]. These investigations were mainly focused on the conventional spherical particles without particular geometries; however, examination of bimetallic alloyed structures with varied shape/morphology that favors to expose specific crystal facets is rarely concerned.

Recently, novel structured Co-based bimetallic materials such as CoPt nanorods [9], CoFe nanocubes [10], CoNi urchins [11], and CoNi nanowires and nanodumbbells [12] have been fabricated in liquid phase by effectively controlling the reduction rate of the metallic ions. In particular, $Co_{80}Ni_{20}$ urchins which were consisted of radiant nanowires have been synthesized by heterogeneous nucleation in polyol, but the length of the wires was limited to about 500 nm [11,12]. We have recently synthesized Co nanowires with a diameter of 10 nm and a length up to 1000 nm by chemical reduction of cobalt acetate using Ru as heterogeneous agent and stearic acid as structure-directing agent [13]. In this work, we have extended to fabricate alloyed CoNi nanowires with this heterogeneous nucleation technique. By varying the basicity of the solution and the loading of Ni in proper ranges, alloyed CoNi nanowires with the diameter of about 10 nm and the length up to 1000 nm were obtained.

2. Experimental

2.1. Materials synthesis

1.0 g of a solid mixture of cobalt and nickel acetate tetrahydrates with desired Ni/Co molar ratios and 0.2 g of sodium hydroxide were dissolved into 80 ml of 1, 2-propanediol. Then, 0.267 g of stearic acid and 0.02 g of $RuCl_3 \cdot xH_2O$ (35 wt% Ru) dissolved in 5 ml of 1, 2-propanediol were added to the solution. The mixture was transferred into a teflon-lined autoclave (100 ml) and gradually heated to 413 K and maintained at this temperature for 12 h. The product was centrifuged, thoroughly washed with ethanol and water, and finally dried at 323 K for 5 h under vacuum. Here, ruthenium is used to facilitate the reduction of cobalt and nickel ions, and stearic acid is to induce the anisotropic growth of the nanocrystals as a structure-directing agent. In order to identify the morphology evolution, the basicity of the synthetic solution was varied by adjusting the concentration of sodium hydroxide from 0.06 to 0.30 M.

2.2. Characterization

Powder X-ray diffraction (XRD) patterns of the samples were recorded on a D/Max-2500/PC diffractometer (Rigaku, Japan) using

* Corresponding author. Tel.: +86 411 84379085; fax: +86 411 84694447.
E-mail address: shen98@dicp.ac.cn (W. Shen).

0167-577X/$ – see front matter © 2010 Elsevier B.V. All rights reserved.
doi:10.1016/j.matlet.2010.03.006

nickel-filtered Cu K_α radiation at 40 kV and 100 mA. Transmission electron microscopy (TEM) images were taken using a Philips Tecnai G^2 Spirit instrument operated at 120 kV. The elemental analysis of the samples was performed by inductively coupled plasma atomic emission spectroscopy (ICP-AES) on a Plasma-Spec-II spectrometer. The N_2 adsorption–desorption isotherm was performed on a Micromeritics ASAP 2010 instrument at 77 K.

2.3. Hydrogenolysis of glycerol

0.05 g of CoNi nanomaterials was added to 40 g of 10 wt% glycerol aqueous solution in an autoclave (100 ml). After purging with hydrogen, the reaction system was pressurized to 3 MPa of hydrogen and heated to 493 K for 7 h under stirring. The products were identified by a mass spectrometer and quantitatively analyzed by a gas chromatography equipped with a flame-ionization detector.

3. Results and discussion

Fig. 1 shows the TEM images of the CoNi materials with varied Ni loading. For Co alone, nanowires with a length of 500–1000 nm and a diameter of about 12 nm were obtained. When 10% Ni was added, the wire-like morphology was maintained, but the diameter decreased to about 7 nm and the length shortened to 200–1000 nm with a cone head of about 50 nm on each tip. It is noted that agglomeration which was mainly composed of the short nanorods with the length of 200–500 nm was also produced. This might be due to the inhomogeneous growth of the CoNi nanocrystals in the stagnant synthetic media, and thus some short rods survived as the final products. When Ni doping was increased to 20%, the nanowires had similar length and diameter as the $Co_{90}Ni_{10}$ sample, but the size of the cone head slightly decreased to about 30 nm. With further increasing Ni loading to 30%, the length of the nanowires was shortened to about 500 nm while the diameter was in the range of 6–12 nm. As 50% Ni was added, however, a mixture of nanorods and aggregated particles was produced. The nanorods had the length of about 500 nm and the diameter of about 20 nm. For pure Ni, only large spherical particles with the size of 50–150 nm were produced, and the particles consisted of nanoplatelets of about 50 nm. Hence, the morphology of the CoNi materials is closely associated with the loading of Ni, and bimetallic nanowires could be obtained when Ni doping was less than 30%.

Fig. 2a shows the XRD patterns of the CoNi materials. Co nanowires exhibited typical diffractions at 2θ values of 41.6°, 44.6°, 47.4° and 62.6°, corresponding to the (100), (002), (101) and (102) planes of hexagonal close-packed structure (JCPDS No. 5-727), respectively. As Ni doping was no more than 30%, the CoNi nanowires had pure hcp phase, but the intensity of the (002) diffraction enhanced gradually with Ni loading, indicating the [002] orientation of these nanowires [13,14]. Meanwhile, the broadening (101) diffraction with increasing Ni doping indicated the presence of a stacking fault [15]. For the $Co_{50}Ni_{50}$ nanorods, in addition to the Co hcp phase, the weak diffraction at 2θ value of 51.6° suggested the presence of face centered cubic Ni phase (JCPDS No. 4-850). This is further confirmed by the intense diffraction at 2θ value of 44.6°, caused by the superposition of the hcp (002) and the fcc (111) planes. As for the Ni aggregates, the intense diffractions at 2θ values of 44.4° and 51.7° clearly indicated the well crystallization of face centered cubic Ni structure. Therefore, Ni doping significantly altered the crystallographic phase of the CoNi materials, and only single hcp Co phase was obtained when the loading of Ni was no more than 30%. Fig. 2b shows the magnified XRD patterns of the (002) planes. It is obvious that the (002) plane shifted from 2θ value of 44.6° (Co) to 44.4° (Ni) with increasing Ni loading, indicating the formation of an alloyed structure. Fig. 2c illustrates that the d-spacing of the (002) plane increased linearly with Ni doping due

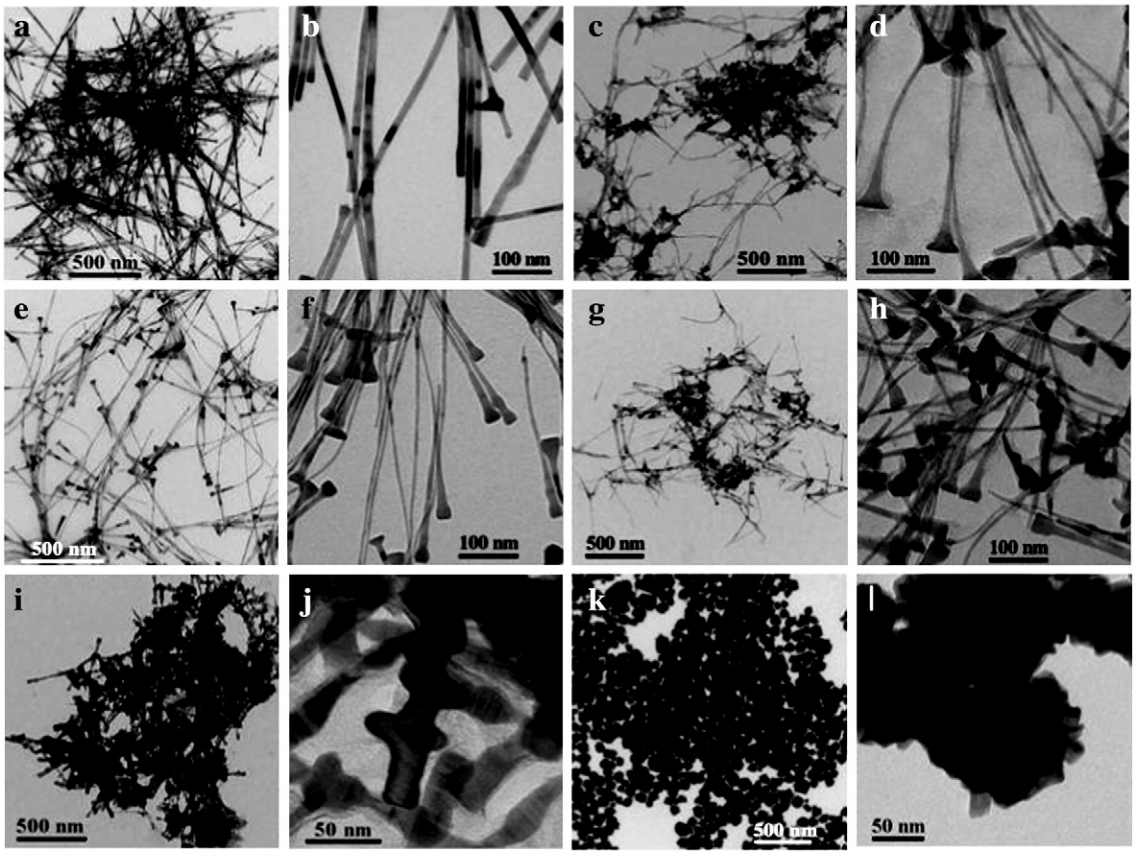

Fig. 1. TEM images of the CoNi nanomaterials: (a–b) Co, (c–d) $Co_{90}Ni_{10}$, (e–f) $Co_{80}Ni_{20}$, (g–h) $Co_{70}Ni_{30}$, (i–j) $Co_{50}Ni_{50}$, and (k–l) Ni.

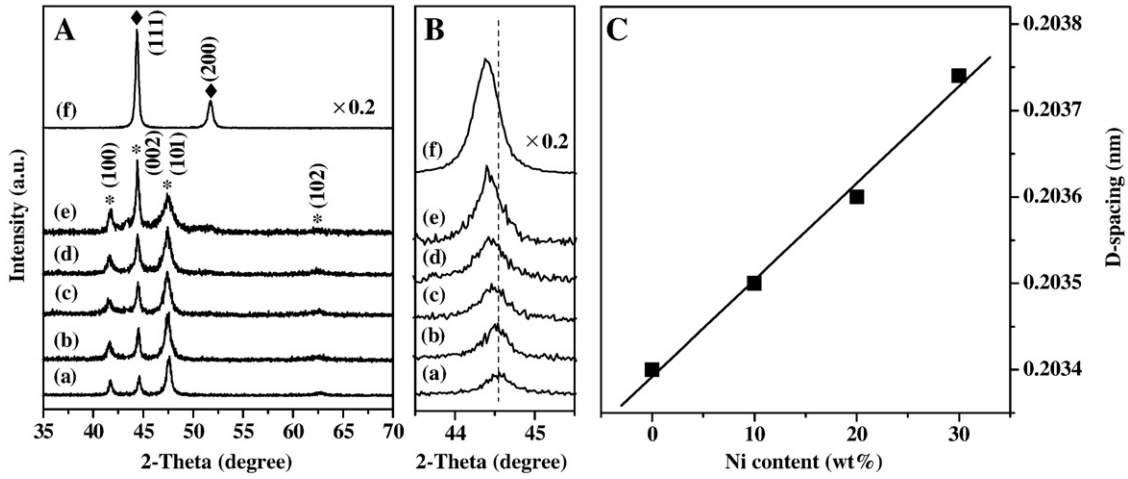

Fig. 2. XRD patterns of the CoNi nanomaterials: (a) Co, (b) $Co_{90}Ni_{10}$, (c) $Co_{80}Ni_{20}$, (d) $Co_{70}Ni_{30}$, (e) $Co_{50}Ni_{50}$, and (f) Ni with the wide diffractions (A), the magnified (002) planes (B), and the d-spacing of the (002) planes (C). (*) and (◆) show the hcp Co and fcc Ni phases, respectively.

to the formation of CoNi alloys [8,16]. Most likely, Ni incorporated into the crystalline lattice of hcp Co and partly replaced Co atoms during the formation of the nanowires because of the closing reduction potentials of Co^{2+} (−0.277 V) and Ni^{2+} (−0.257 V) and thus the similar reduction rates in polyol.

CoNi nanowires with the length of 100–500 nm have been previously synthesized by heterogeneous nucleation in polyols [11,12], cobalt alkoxide and nickel hydroxy-acetate were initially produced as the solid intermediates to reduce the supersaturation of Co^{2+} and Ni^{2+} in the solution, which maintained the balance of nucleation and growth of Co and Ni atoms to form the bimetallic wires. In the current syntheses, stearic acid is used to induce the preferential formation of cobalt and nickel stearate [13]. These new solid intermediates control the anisotropic growth of Co and Ni nanocrystals more efficiently, causing the length of the CoNi wires up to 1000 nm.

Fig. 3 shows the TEM images of the $Co_{90}Ni_{10}$ and $Co_{50}Ni_{50}$ nanomaterials synthesized by varying the basicity of the synthetic solution. For the $Co_{90}Ni_{10}$ materials, nanowires were obtained with the length of 200–1000 nm and the diameter of 7 nm when 0.06 M NaOH was used (Fig. 1). As the concentration of NaOH increased to 0.3 M, the length of the nanowires markedly reduced to 50–100 nm and the diameter decreased to about 3 nm, forming fibrous-like shapes. For the $Co_{50}Ni_{50}$ materials, aggregated nanorods of less than 500 nm in length and about 20 nm in diameter were obtained at lower basicity (0.06 M NaOH), but sphere-like particles with the size of about 10 nm were produced at higher basicity (0.3 M NaOH). It is apparent that the shape of the CoNi materials strongly depends on the basicity of the synthetic solution, and the reducing sizes of both the $Co_{90}Ni_{10}$ nanofibers and the $Co_{50}Ni_{50}$ nanoparticles were caused by the significantly decreased reduction rates of Co^{2+} and Ni^{2+} in strong basic solutions [13,15].

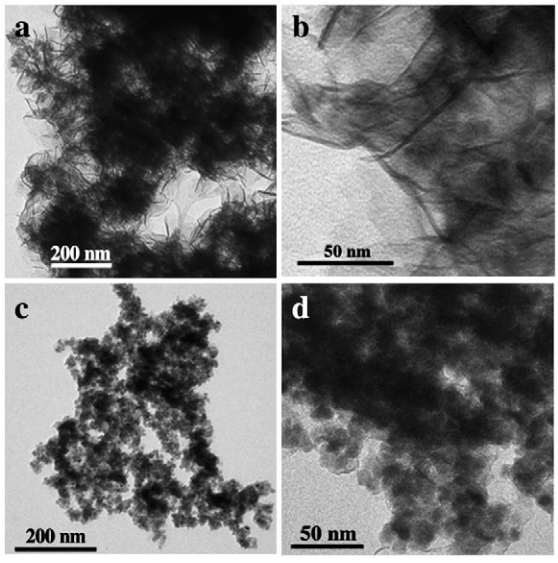

Fig. 3. TEM images of the $Co_{90}Ni_{10}$ (a–b) and $Co_{50}Ni_{50}$ (c–d) nanomaterials synthesized at high basicity (0.3 M NaOH).

When Co^{2+} and Ni^{2+} ions are simultaneously present in polyol, Co^{2+} is initially reduced to Co crystals, followed by the reduction of Ni^{2+} and the remaining Co^{2+} on the surface of Co crystals, forming CoNi nanomaterials [17]. When the loading of Ni is less than 30%, a core-shell like structure with Co as the core and CoNi alloy as the shell is produced. As the loading of Ni is up to 50%, however, the final reduction of Ni^{2+} would deposit on the CoNi alloy surface, showing a mixture of fcc Ni and hcp Co phases. Table 1 summarizes the chemical compositions and the surface areas of the CoNi materials. The Co/Ni molar ratios in the solid products were always higher than those in the initial solutions, and the deviations enlarged with increasing Ni loading. This further confirms that Co^{2+} is initially reduced to Co crystals forming the Co core; the remaining Co^{2+} and Ni^{2+} are only slowly reduced to form the CoNi alloyed shell, and the reduction of the residual Ni^{2+} generates fcc Ni layers on the alloy surface as the Ni doping is more than 30%.

Table 1 compares the catalytic performance of the CoNi nanomaterials for hydrogenolysis of glycerol. The Co nanowires showed 44% glycerol conversion and 60% selectivity to 1, 2-propanediol. When CoNi nanomaterials were used, however, the product spectra were modified considerably. The conversion of glycerol greatly increased to 70% but the selectivity of 1, 2-propanediol decreased to 49% over the

Table 1
Structural and catalytic properties of the CoNi nanomaterials.

Sample	Initial Co/Ni (mol)	Co/Ni (mol)	Surface area (m^2/g)	Glycerol conversion (%)	1, 2-propandiol selectivity (%)
Co nanowires	–	–	25	44	60
$Co_{90}Ni_{10}$ nanowires	9	10.1	36	70	49
$Co_{80}Ni_{20}$ nanowires	4	4.9	23	61	63
$Co_{70}Ni_{30}$ nanowires	2.3	3.3	17	55	62
$Co_{50}Ni_{50}$ nanorods	1	1.7	9	23	67
Ni particles	–	–	12	10	15

$Co_{90}Ni_{10}$ nanowires. With further increasing the doping of Ni, the conversion of glycerol was decreased, whereas the selectivity of 1, 2-propanediol maintained at 61–63%. Concerning the $Co_{0.5}Ni_{0.5}$ nanorods, however, the conversion of glycerol significantly decreased to 23% and the selectivity of propanediol slightly increased to 67%. For Ni particles, the conversion of glycerol and the selectivity of propanediol significantly decreased to 10% and 15%, respectively. Meanwhile, the gas phase products remarkably increased to 73%, mainly because of the high activity of Ni for C–C bond breaking [18].

Obviously, the alloyed CoNi nanowires considerably promoted the conversion of glycerol and the selectivity of propanediol. Probably, the doped Ni modified the electronic properties of Co surface and thus significantly altered the adsorption and activation of glycerol [4,19]. Because the electronegativity of Ni (1.91) is slightly greater than that of Co (1.88), their interaction in the nanowires would cause electron transfer from Co to Ni, possibly forming surface $Co^{\delta+}$ species that facilitate the absorption of glycerol and promote the dehydroxylation of glycerol by weakening the C–O bond [20,21]. However, the activities decreased considerably over the $Co_{50}Ni_{50}$ and Ni catalysts with fcc Ni phase. This further confirms that the reaction occurs mainly on the surface Co, and the covering Ni layers in the $Co_{0.5}Ni_{0.5}$ nanorods blocks the available sites of Co and impeded the hydrogenolysis of glycerol.

4. Conclusion

Alloyed CoNi nanowires were obtained as the loading of Ni was less than 30%. Co^{2+} was initially reduced to Co crystals as the core and the remaining Co^{2+} and Ni^{2+} were slowly and simultaneously reduced to form CoNi alloyed shell. Basicity of the synthetic solution varied the shape of the CoNi nanomaterials considerably through adjusting the reduction rates of the two metal ions. Catalytic test for hydrogenolysis of glycerol revealed that the alloyed CoNi nanowires greatly promoted the catalytic performance, which was much better than the individual Co nanowires and Ni nanoparticles.

References

[1] Toshima N, Yonezawa T. New J Chem 1998;22:1179–201.
[2] Ferrando R, Jellinek J, Johnston RL. Chem Rev 2008;108:845–910.
[3] Rodriguez JA. Surf Sci Rep 1996;24:225–87.
[4] Chen JG, Menning CA, Zellner MB. Surf Sci Rep 2008;63:201–54.
[5] Besenbacher F, Chorkendorff I, Clausen BS, Hammer B, Molenbroek AM, Nørskov JK, et al. Science 1998;279:1913–5.
[6] Knudsen J, Nilekar AU, Vang RT, Schnadt J, Kunkes EL, Dumesic JA, et al. J Am Chem Soc 2007;129:6485–90.
[7] Nagaoka K, Takanabe K, Aika K. Appl Catal A 2004;268:151–8.
[8] Takanabe K, Nagaoka K, Nariai K, Aika KJ. Catal 2005;232:268–75.
[9] Wang Y, Yang H. J Am Chem Soc 2005;127:5316–7.
[10] Kodama D, Shinoda K, Sato K, Konno Y, Joseyphus J, Motomiya K, et al. Adv Mater 2006;18:3154–9.
[11] Ung D, Viau G, Ricolleau C, Warmont CF, Gredin P, Fiévet F. Adv Mater 2005;17:338–44.
[12] Ung D, Soumare Y, Chakroune N, Viau G, Vaulay MJ, Richard V, et al. Chem Mater 2007;19:2084–94.
[13] Guo XH, Liu QY, Li J, Chen JL, Song W, Shen WJ. Nanotechnology 2008;19(365608):1–9.
[14] Hou YL, Kondoh H, Ohta T. Chem Mater 2005;17:3994–6.
[15] Chakroune N, Viau G, Ricolleau C, Fiévet-Vincent F, Fiévet F. J Mater Chem 2003;13:312–8.
[16] Toneguzzo P, Viau G, Acher O, Guillet F, Bruneton E, Fiévet-Vincent F, et al. J Mater Sci 2000;35:3767–84.
[17] Ung D, Viau G, Fiévet-Vincent F, Herbst F, Richard V, Fiévet F. Prog Solid State Chem 2005;33:137–45.
[18] Zhu LJ, Guo PJ, Chu XW, Yan SR, Qiao MH, Fan KN, et al. Green Chem 2008;10:1323–30.
[19] Bertolini JC. Surf Rev Lett 1996;3:1857–68.
[20] Montassier C, Ménézo JC, Hoang LC, Renaud C, Barbier J. J Mol Catal 1991;70:99–110.
[21] Stefanov P. Vacuum 1997;48:69–72.